

# ON THE ORIGIN OF THE CA-TI-CR ISOTOPIC ANOMALIES IN THE INCLUSION EK-1-4-1 OF THE ALLENDE-METEORITE

K.-L. KRATZ<sup>1</sup>, W. BÖHMER<sup>1</sup>, C. FREIBURGHHAUS<sup>2</sup>, P. MÖLLER<sup>3</sup>, B. PFEIFFER<sup>1</sup>,  
T. RAUSCHER<sup>2</sup>, F.-K. THIELEMANN<sup>2</sup>

<sup>1</sup>*Institut für Kernchemie, University Mainz, Fritz-Straßmann-Weg 2  
D-55128 Mainz, Germany*

<sup>2</sup>*Departement für Physik und Astronomie, Universität Basel, Klingelbergstraße 82,  
CH-4056 Basel, Switzerland*

<sup>3</sup>*Theoretical Division, Los Alamos National Laboratory, Los Alamos, NM 87545, USA*

**ABSTRACT.** In the framework of our investigation to explain the nucleosynthetic origin of the correlated Ca-Ti-Cr isotopic anomalies in the Ca-Al-rich "FUN" inclusion EK-1-4-1 of the Allende meteorite, the nuclear-physics basis in the neutron-rich  $N = 28$  region has been updated by including recent experimental data on  $\beta$ -decay properties and microscopic predictions of neutron-capture cross sections. Charged-particle and subsequent r-process calculations within an entropy-based approach were performed using a complete reaction network. It is shown that there exist two astrophysical scenarios within which the observed isotopic anomalies can be reproduced simultaneously; one at low entropies ( $S \simeq 10$ ) which confirms the earlier suggested SN Ia mechanism, and another at high entropies ( $S \simeq 150$ ) which would be compatible with the neutrino-wind scenario of a SN II.

## 1. Introduction

About two decades ago, G.J. Wasserburg and his group at Caltech published two important papers (Lee 1978, Niederer 1980) on the identification of correlated isotopic anomalies for Ca, Ti and Cr in peculiar inclusions of the Allende meteorite. These highly unusual isotopic compositions were attributed to fractionation (F) and unknown nuclear (UN) effects (Lee 1978, Niederer 1980) and therefore designated "FUN" anomalies. It was immediately concluded that those data might provide a clue to the late-stage nucleosynthetic processes which preceded formation of the solar nebula. However, all astrophysical models existing at that time (standard r-process, generic mini r-process, explosive carbon burning, local proton irradiation of solar-system material, nuclear-equilibrium approaches) encountered severe difficulties when they tried to reproduce the observed anomalies of Allende, in particular those of the EK-1-4-1 inclusion; summarized by the – slightly acquiescent – statement of the authors: "*We acknowledge our ignorance of the detailed astrophysical processes...*" (Niederer 1980) which produced the FUN anomalies.

As already suggested by Wasserburg et al. in 1977, a key to a better description of the non-standard abundances may be an improved knowledge of the relevant nuclear-

physics data around doubly-magic  $^{48}\text{Ca}$ . Following this line, in 1982 Sandler, Koonin and Fowler proposed, in their  $n\beta$ -process, specific nuclear-structure properties, i.e. low-lying (30 keV) s-wave neutron-capture resonances, in  $^{46}\text{K}(n,\gamma)$  and  $^{49}\text{Ca}(n,\gamma)$ , respectively, to replace statistical Hauser-Feshbach (HF) cross sections applied in their reaction network. These resonances were deemed necessary to enhance the HF rates by an order of magnitude resulting in a depletion of the above progenitors of  $^{46}\text{Ca}$  and  $^{49}\text{Ti}$ , otherwise being considerably overproduced compared to observation.

## 2. Experiments at CERN/ISOLDE

At this stage, our Mainz–Lund–Garching collaboration became interested in the "EK-1-4-1 story". As nuclear chemists / physicists interested in astrophysics, our specific approach was to systematically investigate the influence of nuclear-structure properties of neutron-rich  $^{16}\text{S}$  to  $^{19}\text{K}$  isotopes on the nucleosynthetic production of their Ca and Ti  $\beta$ -decay daughters. From detailed spectroscopic studies of heavy K isotopes at CERN/ISOLDE, rather surprising results had been obtained, for example a sudden, strong increase of the  $\beta$ -delayed neutron decay branch ( $P_n$ ) from about 1% in  $N = 27$   $^{48}\text{K}$  to 86% in  $N = 28$   $^{49}\text{K}$  (Carraz 1982). In 1985, we reported the experimental identification of the low-lying s-wave resonance for  $J^\pi = 3/2^-$   $^{49}\text{Ca}(n,\gamma)$  (Ziegert 1985b) requested by Sandler et al. (1982), from the "inverse reaction" to neutron capture, i.e. the decay mode of  $\beta$ -delayed neutron emission of 472-ms ( $J^\pi = 0^-$ )  $^{50}\text{K}$ . The  $J^\pi = 1^-$  state was, however, not found at the energy relevant for  $n\beta$ -process temperatures of  $T \simeq 3 - 5 \cdot 10^8$  K, but somewhat higher at 155 keV. Furthermore, subsequent measurements of the partial decay widths of this state (Ziegert 1985a) have put constraints on the Breit-Wigner resonance neutron-capture rate, indicating that it will be roughly equal to the HF rate for the above  $n\beta$ -process temperatures, but may well be larger by up to a factor 7 for  $T \geq 1 \cdot 10^9$ , i.e. for typical r-process temperatures. In any case, our experimental data did not support the  $n\beta$ -explanation of the  $^{49}\text{Ti}$  abundance in EK-1-4-1 suggested by Sandler, Koonin and Fowler (1982).

An extension of this work, using experimental data where available together with improved TDA and QRPA model predictions, definitely excluded the  $n\beta$ -process as a possible astrophysical scenario (Ziegert 1985a, Hillebrandt et al. 1986, Kratz et al. 1991) and favored explosive He-burning in supernovae (SN) with higher neutron exposures of about  $5-7 \cdot 10^{-5}$  mol $\cdot$ cm $^{-3}$  $\cdot$ s as a likely site for the formation of the correlated Ca-Ti-Cr isotopic anomalies in EK-1-4-1. As a consequence of the new nucleosynthesis scenario, other – more exotic – progenitor isotopes became the "key" nuclides to produce only *little*  $^{46}\text{Ca}$  and *much*  $^{48}\text{Ca}$  at the same time, in order to cause the abundance ratio of  $^{48}\text{Ca}/^{46}\text{Ca} \simeq 250$  observed in EK-1-4-1. It was shown that in particular the – at that time still unknown –  $\beta$ -decay half-life of the neutron-magic  $N = 28$  "turning-point" nucleus  $^{44}\text{S}$  (where the neutron-capture half-life becomes comparable to the  $\beta$ -decay half-life;  $T_{1/2}(n) \simeq T_{1/2}(\beta)$ ) would be decisive in defining the neutron-capture process duration, and consequently is determining the final amount of stable  $^{46}\text{Ca}$  (Thielemann et al. 1990). With shell-model predictions for the decay of *spherical*  $^{44}\text{S}$  between 1.1 s (QRPA) and 0.3 s (TDA), the necessary time scale for the neutron irradiation was of the order of 100 ms, and the required abundance of the ( $\alpha,n$ ) neutron source was

$Y_{\alpha,n} \simeq 2 \cdot 10^{-3} \text{ mol}\cdot\text{cm}^{-3}$ . It was well recognized that this might be hard to attain in He-zones of massive stars during a SN explosion. Already in 1979, Thielemann et al. (1979) found that during explosive processing of a  $3\alpha$  layer of standard preshock composition, maximum abundances of  $^{22}\text{Ne}$  (as  $(\alpha,n)$  neutron source) of  $Y_{\text{Ne}} \simeq 10^{-3}$  and resulting free neutrons of  $Y_n \simeq 10^{-9}$  can be realized for the above requested process duration. This was also verified in recalculations with updated reaction rates in 1990 (Thielemann et al. 1990). Due to the strong influence of the neutron poison  $^{25}\text{Mg}$  produced by  $^{22}\text{Ne}(\alpha,n)$ , rather the alternative  $^{18}\text{O}$  and in particular  $^{13}\text{C}$  neutron sources were found to provide the best conditions; however, still at the limit to fulfill the above constraints. Nevertheless, the explosive He-burning scenario was not excluded immediately, because at that time considerable uncertainties still existed in the theoretical nuclear-data input of far-unstable progenitor isotopes. Unfortunately – or ”fortunately” when considering the later, very surprising experimental results presented below – we never published this status of the ”EK-1-4-1 story” in a refereed journal...

### 3. Experiments at GANIL/LISE

In order to eliminate at least some of the remaining uncertainties in the nuclear-structure properties of potential ”turning-point” nuclei south of  $^{48}\text{Ca}$ , in a Mainz–Orsay–Dubna–GANIL collaboration we have performed two experiments at the doubly-achromatic spectrometer LISE of GANIL. As production mechanism, projectile fragmentation of a 60 MeV/u  $^{48}\text{Ca}$  beam was used (Kratz et al. 1991, Sorlin et al. 1993, Kratz et al. 1995, Böhmer 1996). In these experiments, the gross  $\beta$ -decay properties  $T_{1/2}$  and  $P_n$  of the very neutron-rich isotopes  $^{43}\text{P}$ ,  $^{42,44,45}\text{S}$ ,  $^{44-46}\text{Cl}$ , and  $^{47}\text{Ar}$  could be measured for the first time (see Table I). Very surprising results were obtained. Compared to the model predictions used in our earlier astrophysical calculations, which – quite naturally – assumed *spherical* shapes for these  $N \simeq 28$  near-magic nuclides, the experimental  $T_{1/2}$  for most of them (except  $^{44,45}\text{Cl}$ ) were considerably shorter, by about a factor 3 for  $^{43}\text{P}$ ,  $^{42}\text{S}$  and  $^{47}\text{Ar}$ , a factor 4 for  $^{45}\text{Cl}$ , up to a factor 10 for  $^{44,45}\text{S}$ . Similarly, most of the measured  $P_n$  values were unexpected when assuming sphericity. We therefore suggested that our surprising results indicated an erosion of the  $N = 28$  shell-gap below  $^{48}\text{Ca}$  resulting in an onset of strong quadrupole deformation (Sorlin 1993, Kratz et al. 1995). Although initially not predicted by any model of whatever sophistication and therefore not accepted in the nuclear-structure community, our ”unconventional” ideas were rather soon confirmed by both theory and COULEX experiments (see, e.g. Werner 1994, Scheit 1996, Glasmacher 1998).

### 4. Ground-State Shapes from a QRPA Parameter Study

The main motivation for our shell-model parameter study within the quasi-particle random-phase approximation (QRPA) with Folded-Yukawa single-particle (SP) wave functions (Möller and Randrup 1990) was to determine the nuclear shape – spherical or deformed – of the above  $N \simeq 28$  isotopes exclusively from a comparison of their experimental and calculated gross  $\beta$ -decay properties  $T_{1/2}$  and  $P_n$  (Böhmer 1996). These quantities were calculated as functions of quadrupole deformation, where the  $\epsilon_2$ -parameter

TABLE I

QRPA-calculation of  $T_{1/2}$  and  $P_n$  with optimized ground-state quadrupole deformation of the investigated nuclei. In column 2, the deformation parameter  $\epsilon_2$  is given which leads to the best agreement between the calculated  $T_{1/2}$  and  $P_n$  values (columns 3 and 4) and the experimental results (columns 5 and 6).

Isotope	Optimized $\epsilon_2$	Theoretical values		Experimental values	
		$T_{1/2}$ [ms]	$P_n$ [%]	$T_{1/2}$ [ms]	$P_n$ [%]
$^{43}\text{P}$	-0,175	70	100,0	$36\pm 4$	$100\pm 10$
$^{42}\text{S}$	-0,300	1300	0,9	$579\pm 46$	<4
	+0,300	1570	0,1		
$^{44}\text{S}$	+0,325	133	15,3	$123\pm 10$	$18\pm 3$
$^{45}\text{S}$	-0,200	83	39,8	$72\pm 5$	$54\pm 6$
	+0,125	90	36,7		
$^{44}\text{Cl}$	-0,250	434	1,8	$438\pm 19$	<8
$^{45}\text{Cl}$	-0,200	392	10,4	$412\pm 39$	$38\pm 5$
$^{46}\text{Cl}$	+0,100	204	57,9	$223\pm 37$	$60\pm 9$
$^{47}\text{Ar}$	-0,180	705	0,1	$613\pm 197$	<1
	+0,125	709	0,1		

was varied in small steps between -0.35 and +0.35, i.e. between strongly oblate and strongly prolate.

The nuclei considered in this study, have 15 to 18 protons and 26 to 30 neutrons. In this low-mass region the single-proton and single-neutron levels are well separated by 1–5 MeV (see, e.g. the Folded-Yukawa SP-diagrams in Möller 1997). For both protons and neutrons, pronounced spherical shell-gaps exist for particle numbers 14, 20 and 28, and deformed gaps develop around  $\epsilon_2 \simeq +0.2$  for particle numbers 16, 26 and 30 and around  $\epsilon_2 \simeq -0.25$  for particle number 18, replacing the above spherical shell-gaps. In any case, more or less independent of the nuclear shape, the low SP-level densities together with the  $\beta$ -decay selection rules yield only a few Gamow-Teller (GT) transitions. In fact, in the  $A \simeq 45$  mass region considered here, the quantities  $T_{1/2}$  and  $P_n$  are to a large extent determined by one or two strong GT-transitions in the respective energy intervals, whereas the effects of forbidden transitions can be neglected. Thus, the expected correlation between the gross  $\beta$ -decay properties and the nuclear shape should be unambiguous, at least to distinguish between sphericity and collectivity.

In the following, let us exemplarily discuss the results and their relation to our astrophysical "turning-point" nucleus  $^{44}\text{S}$ . According to the prediction of most global models, the neutron-magic nucleus  $^{44}\text{S}$  should be spherical in its ground state. A QRPA calculation in the spherical limit leads to a rather long half-life of  $T_{1/2} = 1.12\text{s}$  and a maximum possible neutron emission probability of  $P_n = 100\%$  (Sorlin 1993, Kratz et al. 1995). In this case, the two (lowest-energy)  $\nu f_{7/2} \rightarrow \pi f_{7/2}$  GT-transitions determining both gross  $\beta$ -decay properties lie above the neutron separation energy, at about 5 MeV in the daughter nucleus  $^{44}\text{Cl}$ . Much better agreement with the experimental values of  $T_{1/2} = (123 \pm 10)$  ms and  $P_n = (18 \pm 3)\%$  are obtained if we perform the QRPA cal-

calculation with a prolate deformation of  $\epsilon_2 \simeq 0.3$ . For this shape, GT-transitions between deformed Nilsson-orbitals of  $f_{7/2}$  shell-model origin are shifted down in energy to near the ground state of  $^{44}\text{Cl}$ , resulting in a shorter half-life of  $T_{1/2}=133$  ms together with a lower  $\beta$ -delayed-neutron emission probability of  $P_n = 15.3\%$ . From this comparison, one clearly can exclude the spherical shape for  $^{44}\text{S}$ . As mentioned above, in the meantime our conclusion has been confirmed by intermediate-energy Coulomb excitation experiments of B(E2)-values (Scheit 1996, Glasmacher 1998).

In the same way, the results on the non-spherical ground-state shapes for the other  $N \simeq 28$  nuclei were obtained. Table I summarizes the deformation parameters for which our QRPA calculations yielded the best agreement with the experimental values. In a number of cases, e.g. for  $^{42,45}\text{S}$  and  $^{47}\text{Ar}$ , our approach is not able to determine whether these isotopes are prolate or oblate deformed, but can again exclude a spherical shape. This general distinction between collectivity and sphericity is, however, of major importance as input for improved predictions of neutron-capture cross sections (Rauscher et al. 1998) entering our astrophysical network calculations discussed below.

## 5. Theoretical Neutron-Capture Rates

Apart from nuclear masses and  $\beta$ -decay properties, also neutron-capture cross sections ( $\sigma_n$ ) are important input data for calculations of non-equilibrium r-process-like nucleosynthesis scenarios. For typical astrophysical neutron energies, two reaction mechanisms have to be considered (Rauscher 1995): (i) Capture reactions where a *compound nucleus* (CN) is created; in this case  $\sigma_n(\text{CN})$  values are commonly calculated with the statistical Hauser-Feshbach model. (ii) Reactions where a neutron is directly captured into bound states, i.e. *direct capture*, (*DC*). The DC-mechanism can dominate the neutron-capture for nuclei with low level density in the vicinity of the neutron separation energy  $S_n$ . This is especially the case for light-mass nuclei, for isotopes close to magic neutron numbers, and for nuclei far from  $\beta$ -stability with low  $S_n$  values. Therefore, in the present study, in addition to CN cross sections (Rauscher et al. 1998) also the DC contributions of all even-even (ee) nuclei (because of level-density arguments one can assume to first order that DC will be more important for capture on ee targets than on odd-nucleon ones) between  $^{40}\text{S}$  to  $^{74}\text{Fe}$  were calculated with the code TEDCA, as follows.

The theoretical cross section  $\sigma^{th}$  is given by a sum over each final state  $i$  (Kim et al. 1987)

$$\sigma^{th} = \sum_i C_i^2 S_i \sigma_i^{DC} \quad . \quad (1)$$

In our case the isospin Clebsch-Gordan coefficients  $C_i$  are equal to unity. The spectroscopic factors  $S_i$  describe the overlap between the antisymmetrized wave functions of target+n and the final state. In the case of one-nucleon capture on even-even deformed nuclei, the spectroscopic factor for capture into a state  $i$ , which has an occupation probability  $v_i^2$  in the target, can be reduced to (Glendenning 1983)

$$S_i = 1 - v_i^2 \quad . \quad (2)$$

The corresponding probabilities  $v_i^2$  are found by solving the Lipkin-Nogami pairing equations (Möller 1995).

The factors  $\sigma_i^{DC}$  in Eq. 1 are essentially determined by the overlap of the scattering wave function in the entrance channel, the bound-state wave function and the multipole-transition operator. The potentials needed for the calculation of the before-mentioned wave functions are obtained by applying the folding procedure. In this approach, the nuclear density of the target  $\rho_T$  is folded with an energy and density dependent effective nucleon-nucleon interaction  $w_{eff}$  (Kobos et al. 1984)

$$V(E, R) = \lambda V_F(E, R) = \lambda \int \rho_T(\mathbf{r}) w_{eff}(E, \rho_T, |\mathbf{R} - \mathbf{r}|) d\mathbf{r} \quad , \quad (3)$$

with  $\mathbf{R}$  being the separation of the centers of mass of the two colliding nuclei. The interaction  $w_{eff}$  is only weakly energy dependent in the energy range of interest (Oberhammer and Staudt 1991). The density distributions  $\rho_T$  were calculated from the folded-Yukawa wave functions.

The only remaining parameter  $\lambda$  was determined by employing a parametrization of the volume integral  $I$

$$I(E) = \frac{4\pi}{A} \int V_F(R, E) R^2 dR \quad , \quad (4)$$

expressed in units of  $\text{MeV fm}^3$ , and with the mass number  $A$  of the target nucleus. Recently, the averaged volume integral  $I_0$  was fitted to a function of mass number  $A$ , charge  $Z$  and neutron number  $N$  for a set of specially selected nuclei: (Balogh 1994, Krausmann et al. 1996)

$$I_0 = 255.13 + 984.85A^{-1/3} + 9.52 \cdot 10^6 \frac{N - Z}{A^3} \quad . \quad (5)$$

Thus, the strength factor  $\lambda$  can easily be computed for each nucleus by using

$$\lambda = \frac{I_0}{I} \quad . \quad (6)$$

For the bound states, the parameters  $\lambda$  are fixed by the requirement of a correct reproduction of the separation energies.

The calculated CN and DC cross sections as well as the deformation parameters used for the calculation of the single-particle levels are shown in Table II. Experimentally known neutron separation energies in the final nuclei were taken from a recent data compilation (Audi and Wapstra 1993); otherwise predictions from the finite-range droplet mass model FRDM (Möller 1995) were used. Furthermore, in this table  $\beta$ -decay half-lives ( $T_{1/2}(\beta)$ ) are compared to theoretical lifetimes for neutron capture ( $T_{1/2}(n)$ ). Experimental  $T_{1/2}(\beta)$  were again taken from recent compilations (Audi and Wapstra 1993, Pfeiffer et al. 2000), and – where necessary – theoretical values were obtained by using the QRPA code of Möller and Randrup (1990). The  $T_{1/2}(n)$  were computed from our present DC+CN results with neutron number densities of  $3 \cdot 10^{19} \text{ cm}^{-3}$  for S and Ar target isotopes and  $6 \cdot 10^{20} \text{ cm}^{-3}$  for Ti, Cr and Fe isotopes, respectively. For the Ca

TABLE II

Calculated 30-keV (c.m.) Maxwellian averaged neutron-capture cross sections  $\langle \sigma \rangle_{30 \text{ keV}}$  for CN and DC. The column labeled “%” gives the fraction of direct capture in the total cross section. Also shown are the deformation parameters  $\epsilon_2$  and the neutron separation energies  $S_n$  of the final nuclei, target+n. The neutron-capture half-lives  $T_{1/2}(n)$  were computed with the values from column “DC+CN” and neutron number densities of  $3 \cdot 10^{19}$  for S and Ar target isotopes, and  $6 \cdot 10^{20} \text{ cm}^{-3}$  for Ti, Cr and Fe isotopes, respectively. The values for the Ca isotopes were taken from an earlier calculation using the same model (Krausmann et al. 1996).

Target	$\epsilon_2$	$S_n$ [MeV]	DC [mb]	CN [mb]	DC+CN [mb]	%	$T_{1/2}(n)$ [s]	$T_{1/2}(\beta)$ [s]
<sup>40</sup> S	+0.24	3.8238 <sup>‡</sup>	0.4246	0.0851	0.5097	83	0.218	8.8±2.2 <sup>†</sup>
<sup>42</sup> S	+0.30	3.3114 <sup>‡</sup>	0.9466	0.0202	0.9668	98	0.115	0.579±0.046 <sup>†</sup>
<sup>44</sup> S	+0.30	1.3344	0.014	0.0044	0.0184	76	6.040	0.123±0.010 <sup>†</sup>
<sup>46</sup> Ar	-0.18	4.2590 <sup>‡</sup>	0.5295	0.1203	0.6498	81	0.171	8.4±0.6 <sup>†</sup>
<sup>48</sup> Ar	-0.22	1.7074	0.0427	0.0144	0.0571	75	1.946	0.11
<sup>50</sup> Ar	-0.28	1.0804	0.0016	0.0030	0.0046	35	24.15	0.05
<sup>56</sup> Ti	+0.13	2.1936 <sup>‡</sup>	0.0147	0.1305	0.1452	10	0.038	0.15±0.03 <sup>†</sup>
<sup>58</sup> Ti	-0.10	2.4244	0.0185	0.0797	0.0982	19	0.057	0.047±0.010 <sup>†</sup>
<sup>60</sup> Ti	-0.02	2.1194	0.0165	0.0403	0.0568	29	0.098	0.054
<sup>62</sup> Ti	-0.04	0.5878	0.0068	0.0030	0.0098	69	0.569	0.018
<sup>64</sup> Ti	+0.06	0.4094	0.0013	0.0002	0.0015	87	3.561	0.039
<sup>66</sup> Ti	+0.14	0.3914	0.0009	0.0002	0.0011	82	4.960	0.013
<sup>62</sup> Cr	+0.30	2.9134	0.0119	0.3846	0.3965	<1	0.014	0.187±0.015 <sup>†</sup>
<sup>64</sup> Cr	+0.05	1.8614	0.0170	0.0353	0.0523	33	0.106	0.044±0.012 <sup>†</sup>
<sup>66</sup> Cr	+0.10	2.2374	0.0126	0.0673	0.0799	16	0.071	0.071
<sup>68</sup> Cr	+0.16	1.8274	0.0129	0.0268	0.0397	32	0.140	0.026
<sup>72</sup> Fe	+0.14	2.2474	0.0101	0.0572	0.0673	15	0.083	0.089
<sup>74</sup> Fe	+0.07	2.0564	0.0104	0.0360	0.0464	22	0.120	0.052
<sup>76</sup> Fe	+0.06	0.0584	0.0050	$3 \cdot 10^{-6}$	0.0050	>99	1.12	0.045

<sup>†</sup> experimental  $\beta$ -decay half-life (Audi and Wapstra 1993, Pfeiffer et al. 2000)

<sup>‡</sup> experimental  $S_n$  value (Audi and Wapstra 1993)

nuclides, the values were calculated earlier by Krausmann et al. (1996) with the same model.

From Table II one can see nicely the importance of direct capture when approaching the magic neutron number  $N = 28$  (S, Ar), but also the increasing contribution of DC to the total cross section when approaching the neutron drip-line. As already mentioned above, “*turning-points*” are reached in our r-process scenario for those isotopes where the half-life for capturing the next neutron becomes longer than the  $\beta$ -decay lifetime. Consequently, the nuclear-physics properties of  $N = 28$  <sup>44</sup>S,  $N = 30$  <sup>48</sup>Ar,  $N = 36$  <sup>58</sup>Ti,  $N = 40$  <sup>64</sup>Cr and  $N = 48$  <sup>74</sup>Fe are of primary importance.

## 6. Astrophysical Network Calculations

In the late phase of massive stars, prior to the occurrence of rapid neutron-capture nucleosynthesis, reactions with charged particles such as  $(p,\gamma)$ ,  $(p,n)$ ,  $(\alpha,n)$  and  $(\alpha,\gamma)$ , as well as their inverse reactions,  $\beta^+$ -decays and electron captures take place at high temperatures of  $T_9 \geq 3$ . The process paths as well as the development of the stars can be studied in full network calculations nowadays. The reliability of such calculations depends, among other things, also on the sophistication and internal consistency of the nuclear-physics input of the involved isotopes. Hence, in our nucleosynthesis calculations all nuclear input data, such as masses, neutron-separation energies, level-energies, their spin and parity, the ground-state shape, neutron-capture cross sections and decay-properties were taken into account. If available, experimental data were used, otherwise the input data were obtained from large-scale calculations using modern macroscopic-microscopic models.

As already pointed out in the introduction, the essential goal of our present investigation was to find a realistic nucleosynthesis process which reproduces simultaneously the complete Ca–Ti–Cr isotopic FUN anomalies observed in the EK-1-4-1 inclusion. The required stellar parameters, in particular neutron density ( $\rho_n$ ), radiation-entropy ( $S \propto T_9^3/\rho$ ) and time scale of the process ( $\tau$ ), are then expected to give tight constraints on the possible astrophysical conditions within the chosen scenario. As in Freiburghaus et al. (1999), our calculations follow a hot blob of matter with entropy  $S$ : (1) Initially, it consists of neutrons, protons and some  $\alpha$ -particles in a ratio given by nuclear statistical equilibrium (NSE) for a specific proton-to-nucleon ratio  $Y_e$ , and expands adiabatically and cools from  $T_9 \simeq 9$  to freeze-out conditions of  $T_9 \simeq 1$ . (2) Thereby, the nucleons and  $\alpha$ -particles combine to heavier nuclei (typically Fe group), with some free neutrons and  $\alpha$ -particles remaining. (3) For high entropies, an  $\alpha$ -rich freeze-out from charged-particle reactions occurs for declining temperatures, producing nuclei in the mass range  $A \simeq 80$ –100. (4) Finally, below  $T_9 \simeq 3$  these nuclei can capture the remaining neutrons and undergo r-process-like processes. We consider a simple model of an adiabatically expanding homogeneous mass zone with an expansion timescale relevant to the supernova problem. It is generally accepted now that this approximation is justified by hydrodynamic and semi-analytical simulations of the evolution of the high-entropy wind of a SN. The calculations were performed for a grid of entropies ( $S = 3, 10, 20, \dots, 300 k_B/\text{baryon}$ ) and proton-to-nucleon ratios ( $Y_e = 0.42, 0.45, 0.48$ ), the latter "measuring" the neutron-richness of the initial composition.

Because of the chronological order of the so-called  $\alpha$ -process and a neutron-capture process in the late phase of a massive star, our computer-code was organized in two steps. That part of the network which calculates the charged-particle reactions, was developed by F.-K. Thielemann (1990) and extends from  ${}^1\text{H}$  to  ${}_{46}\text{Pd}$ . On the neutron-rich side all nuclei up to the neutron-drip line were included. On the proton-rich side, only the first three isotopes away from  $\beta$ -stability were taken into account. After the initial calculations of the  $\alpha$ -process, subsequent calculations were performed with the r-process code from C. Freiburghaus for those cases where one or more free neutrons per seed-nucleus ( $Y_n/Y_{\text{seed}} \geq 1$ ) were still existing. A detailed description of the physical processes and the necessary system of equations is given in (Freiburghaus 1999). These r-process



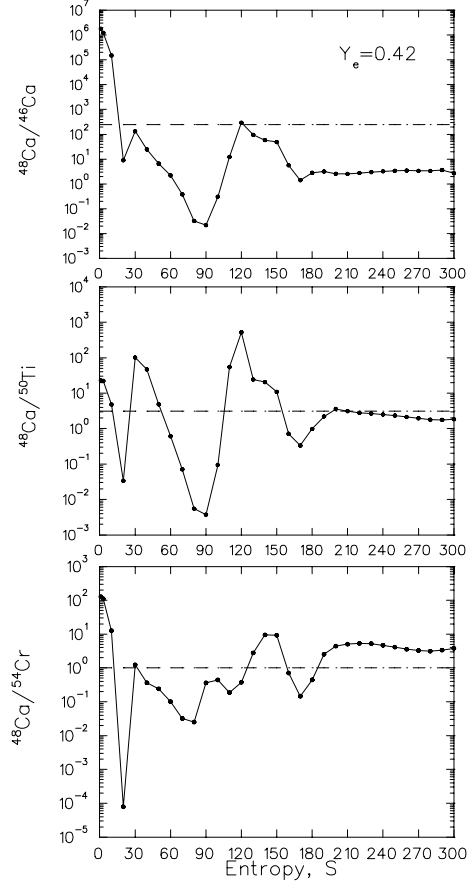


Fig. 1. Calculated isotope abundance ratios of  $^{48}\text{Ca}/^{46}\text{Ca}$ ,  $^{48}\text{Ca}/^{50}\text{Ti}$  and  $^{48}\text{Ca}/^{54}\text{Cr}$  as a function of entropy. Here, a proton-to-nucleon ratio of  $Y_e = 0.42$  has been chosen. The dashed lines represent the respective abundance ratios observed in the EK-1-4-1 inclusion of the Allende meteorite.

calculations are fully dynamical and are not restricted to a  $(n,\gamma)$ - $(\gamma,n)$  equilibrium, as were former calculations.

### 6.1. Isotope Abundances as a Function of Entropy

In Fig. 1 the calculated isotope abundance ratios for  $^{48}\text{Ca}/^{46}\text{Ca}$ ,  $^{48}\text{Ca}/^{50}\text{Ti}$  and  $^{48}\text{Ca}/^{54}\text{Cr}$  at  $Y_e = 0.42$  are displayed as a function of entropy ( $3 \leq S \leq 300$ ). The dashed lines represent the values observed in EK-1-4-1; i.e.  $^{48}\text{Ca}/^{46}\text{Ca} \simeq 250$ ,  $^{48}\text{Ca}/^{50}\text{Ti} \simeq 3$ , and  $^{48}\text{Ca}/^{54}\text{Cr} \simeq 1$ . The isotopes  $^{48}\text{Ca}$ ,  $^{50}\text{Ti}$  and  $^{54}\text{Cr}$  are the most neutron-rich stable ones for each element, and all three are significantly overabundant compared to "normal" solar matter. Moreover, even their ratios among each other are enriched in  $^{48}\text{Ca}$  by

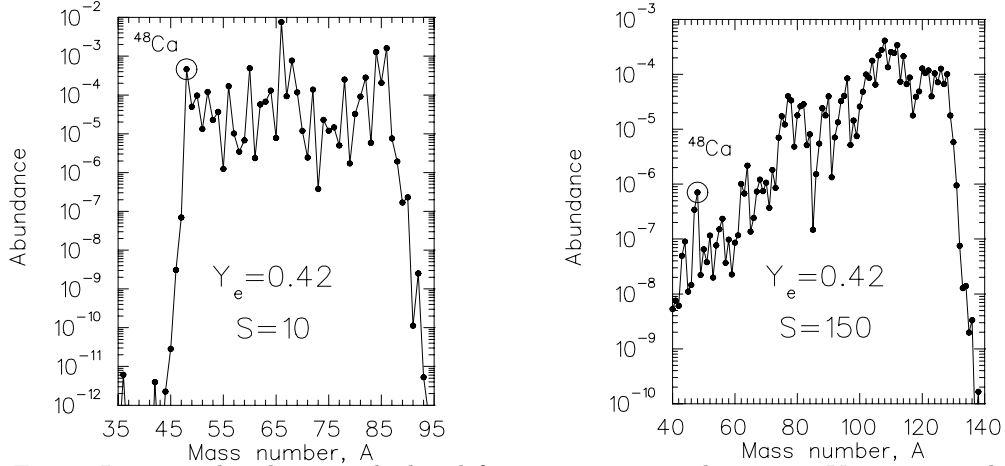


Fig. 2. Isotopic abundances calculated for a proton-to-nucleon ratio  $Y_e = 0.42$  and entropies of  $S = 10 k_B/\text{baryon}$  (left part) and  $S = 150 k_B/\text{baryon}$  (right part).

factors of 3–4 compared to solar. Therefore, over and above a reproduction of the abundances of the stable isotopes within each Z-chain, the most sensitive test of our entropy-based model will be the above abundance ratios.

As can be seen from Figure 1, there are two entropy regions for which these isotope abundance ratios in EK-1-4-1 can be reproduced, one at low entropies ( $S \simeq 10 k_B/\text{baryon}$ ) and the other at high entropies ( $S \simeq 150 k_B/\text{baryon}$ ). In the first case, the Ca–Ti–Cr isotopes are synthesized in an  $\alpha$ -rich freeze-out where essentially no free neutrons are available for subsequent neutron captures. Hence, the neutron-rich stable isotope  $^{48}\text{Ca}$ , for example, is formed *directly*. This is in agreement with the earlier study of Meyer, Krishnan and Clayton (Meyer 1996). In the second case, already some amount of free neutrons exists that can start a kind of weak r-process after the charged-particle freeze-out. Under such conditions,  $^{48}\text{Ca}$  is mainly generated by  $\beta$ -decay of its progenitor  $^{48}\text{Ar}$ . And  $^{44}\text{S}$ , indeed, acts as a “*turing-point*” nucleus, thus avoiding the production of large amounts of  $^{46}\text{S}$  the main progenitor of stable isobaric  $^{46}\text{Ca}$ .

It may be of further interest to compare the whole abundance distributions produced under the above two entropy conditions (see Fig. 2). In principal agreement with the results obtained by Freiburghaus et al. (1999), for low entropies sizeable abundances from the freeze-out of an  $\alpha$ -rich Si-QSE (quasi nuclear statistical equilibrium) are obtained only in a limited mass range; i.e. within  $45 \leq A \leq 95$ . For higher entropies, abundances from the freeze-out of a neutron-rich Fe-QSE extend up to heavier masses. They show an increasing pattern from  $A \simeq 40$  to  $A \simeq 120$ , with a sudden drop around  $A \simeq 130$  where the neutron-capture path reaches  $N = 82$  neutron-magic isotopes. There are also considerable differences in the absolute abundances of the two scenarios, shown in Fig. 2 in the units of the solar Si abundance ( $\text{Si} = 10^6$ ). At low entropies, the even-even Ca–Ti–Cr isotopes of interest are produced at a level of about  $10^{-4}$ , whereas for the higher entropies they lie roughly three orders of magnitude lower.

It may also be of interest to consider abundance ratios of e.g.  $^{48}\text{Ca}$  with heavier neutron-rich stable isotopes expected – and, indeed, partly observed in CaAl-rich inclusions – to be overabundant compared to solar, such as  $^{58}\text{Fe}$ ,  $^{64}\text{Ni}$ ,  $^{66}\text{Zn}$  and  $^{96}\text{Zr}$ . As may already be inferred from a fleeting glance of Fig. 2, there are large differences for the low- and high-entropy scenarios. If some tiny amount of EK-1-4-1 material could still be found, those different abundance patterns might motivate further experimental studies with today's much more sensitive techniques. To give an example, in case of the formation of the Ca–Ti–Cr abundances in a Si-QSE (see, S=10) the abundance ratios of  $Y(^{90-96}\text{Zr})/Y(^{48}\text{Ca})$  should lie between  $5\cdot 10^{-4}$  and  $5\cdot 10^{-10}$ , i.e. *negligible*, whereas for an Fe-QSE followed by a weak r-process (S=150) the above ratios would be orders of magnitude larger (in detail, 56, 1.7, 11, 45, 120 for  $^{90,91,92,94,96}\text{Zr}$ , respectively). Under these latter conditions, the calculated  $Y(^{91,92}\text{Zr})/Y(^{90}\text{Zr})$  isotopic ratios would be exactly the solar r-abundance ( $Y_{r,\odot}$ ) ratios (Käppeler et al. 1989, Arlandini et al. 1999), whereas the  $^{94,96}\text{Zr}/^{90}\text{Zr}$  ratios already show considerable overabundances of the heaviest Zr isotopes compared to  $Y_{r,\odot}$  by factors of about 8 and 12, respectively.

In the context of the question, which of our two nucleosynthesis scenarios – the low- or the high-entropy approach – has most likely produced the FUN anomalies in EK-1-4-1, it is interesting to remember that in fact the very first measurements were made for Ba, Nd and Sm (Lugmair et al. 1978, McCulloch and Wasserburg 1978a, 1978b). They found excesses of the unshielded heaviest isotopes, which are generally believed to be pure r-process products. Within our entropy-based parameter study, only the high-entropy scenario is able to produce isotopes beyond  $A\simeq 130$  with measurable abundances ( $Y(Z\geq 56)\geq 10^{-10}$ ). At the example of the Sm isotopic ratios, relative to r-only  $^{149}\text{Sm}$ , in Table III we compare the weighted averages of the experimental values obtained by Lugmair et al. (1978) and McCulloch and Wasserburg (1978) for EK-1-4-1 with those of the solar-system s- and r-process abundances and our predictions for different entropies in the range S=150–230. It is immediately evident that the measured EK-1-4-1 values are undoubtedly not of s-process origin; however, they are also not fully compatible with the entropy- (neutron-density) mix required to explain the  $Y_{r,\odot}$  pattern. Our calculations show that an r-process-like scenario with a *limited range* of entropies is able to reproduce the observed values. When starting with S=150, the absolute abundance of  $^{149}\text{Sm}$  is of the order of  $Y(^{149}\text{Sm})\simeq 2\cdot 10^{-13}$  and seems to be still overproduced, whereas the two heaviest Sm isotopes are still underproduced relative to EK-1-4-1. This picture changes gradually with increasing entropies. The absolute abundances of all Sm nuclides increase up to S $\simeq$ 210 (e.g.,  $Y(^{149}\text{Sm})\simeq 4\cdot 10^{-10}$  for S=170,  $3\cdot 10^{-7}$  for S=190,  $1\cdot 10^{-5}$  for S=210) and then decrease again. In parallel, with increasing entropy more and more r-material is shifted to the heavier Sm isotopes. This is clearly reflected by the abundance ratios  $Y(^{152,154}\text{Sm})/Y(^{149}\text{Sm})$  in the table. Not only when considering the ratios, but also when using the *absolute* Sm abundances *best* agreement with EK-1-4-1 is obtained around S $\simeq$ 190–200. These are conditions just at the upper end of the high-entropy region where also the correlated Ca–Ti–Cr anomalies in this inclusion could be reproduced. It is worth to be mentioned in this context, that a quite similar picture is observed for the Nd isotopic abundance ratios measured by Lugmair et al. (1978) and McCulloch and Wasserburg (1978 a). A more detailed exploration of the astrophysical conditions to produce those isotopes in EK-1-4-1 and other meteoritic

TABLE III

Comparison of Sm isotopic abundance ratios observed in EK-1-4-1 (Lugmair et al. 1978, McCulloch and Wasserburg 1978b) with solar-system s- and r-process abundances, and with our network calculations for different entropies.

Isotope abund.-ratio	$Y_{s,\odot}$ <sup>a)</sup>	$Y_{r,\odot}$ <sup>b)</sup>	$Y_{EK-1-4-1}$ <sup>c)</sup>	Network calculations				
				S=150	S=170	S=190	S=210	S=230
$^{147}\text{Sm}/^{149}\text{Sm}$	1.92	1.01	$0.99\pm 0.10$	3.05	1.82	1.23	0.93	0.87
$^{152}\text{Sm}/^{149}\text{Sm}$	3.50	1.71	$0.74\pm 0.10$	0.25	0.22	0.77	2.18	2.18
$^{154}\text{Sm}/^{149}\text{Sm}$	0.088	1.87	$1.00\pm 0.11$	0.035	0.16	0.47	1.54	1.81

<sup>a)</sup> Käppeler et al. 1990

<sup>b)</sup> Arlandini et al. 1999

<sup>c)</sup> Lugmair et al. 1978, McCulloch and Wasserburg 1978b

inclusions is presently underway and will be published elsewhere.

## 6.2. Possible Astrophysical Scenarios

We have shown that resultant abundances of neutron-rich stable isotopes in the  $^{48}\text{Ca}$  to  $^{66}\text{Zn}$  region can be produced in matter expanding from high temperature and density for two different entropy regions. In agreement with Meyer et al. (Meyer 1996), we find that for low entropies ( $S \simeq 10 k_B/\text{baryon}$ ) these isotopes are synthesized in the  $\alpha$ -rich freeze-out from a Si-QSE. In this case, the key nucleus  $^{48}\text{Ca}$  is synthesized *directly* without significant neutron captures. Such conditions are found in Type Ia supernovae (SN Ia), which are certainly responsible for the production of the "bulk"  $^{48}\text{Ca}$  material in our solar system, as outlined by Meyer, Krishnan and Clayton.

We have furthermore shown that the Ca–Ti–Cr anomalies in EK-1-4-1 can also be reproduced with higher entropies of  $S \simeq 150\text{--}190 k_B/\text{baryon}$ , however with considerably lower yields than with low entropies. Under these conditions, neutron-rich matter is formed by the freeze-out of an  $\alpha$ -rich Fe-QSE with subsequent r-process-like neutron captures. In this case, the abundance distribution is much larger and ranges up to the rare-earth region. A realistic astrophysical site for such a scenario would be the high-entropy bubble at the outer core of a type II supernova (SN II). Meyer et al. (1996) conclude from their detailed NSE network calculations that  $^{48}\text{Ca}$  does not survive such an environment, because the material freezes out with too few nuclei at low masses. In their model, the QSE nearly exclusively produces nuclei heavier than  $^{48}\text{Ca}$ ; therefore, they make the rather strong statement: "*We therefore rule out this Type II site as an origin for  $^{48}\text{Ca}$ , even in matter having the neutron richness of  $^{48}\text{Ca}$ .*". Here, we disagree with Meyer et al. (1996). In our network calculations, maybe due to the considerably improved nuclear-physics data input for neutron-rich isotopes, we still obtain measurable quantities of nuclides in the  $^{48}\text{Ca}$  region *simultaneously* with overabundances of the heaviest stable isotopes up to Nd and Sm, also observed in EK-1-4-1 (Lugmair et al. 1978, McCulloch and Wasserburg 1978a,1978b). Typical yields for low-mass isotopes

with  $S=150 k_B/\text{baryon}$  are  $1 \cdot 10^{-10} M_\odot$  for  $^{46}\text{Ca}$ ,  $4 \cdot 10^{-8} M_\odot$  for  $^{48}\text{Ca}$ ,  $2 \cdot 10^{-9} M_\odot$  for  $^{50}\text{Ti}$  and  $3 \cdot 10^{-8} M_\odot$  for  $^{54}\text{Cr}$ . This is about 2 to 3 orders of magnitude less than in SN Ia. Moreover, SN II events occur approximately ten times less than SN Ia. Taken together, the contribution of synthesized and ejected matter from SN II is a factor  $10^3$  to  $10^4$  less than the "bulk" material from SN Ia. Hence, we absolutely agree with Meyer et al. (1996), that SN II do not produce enough low-mass material to generate the solar amounts of  $^{48}\text{Ca}$ ,  $^{50}\text{Ti}$  and  $^{54}\text{Cr}$ . However, the amount of matter ejected by Type II supernovae may well be sufficient to explain the observations in the specific SN condensate EK-1-4-1. In an attempt to explain the correlation of overabundances of neutron-rich isotopes over a wide range of elements in CaAl-rich inclusions, Meyer et al. (1996) argue that this material, which was formed in the solar accretion disk, contains "components not only from many Type Ia supernovae but from Type II supernovae as well.". In our high-entropy approach, however, **all** FUN anomalies, from  $^{48}\text{Ca}$  up to  $^{154}\text{Sm}$  observed in EK-1-4-1, are produced simultaneously in the high-entropy bubble scenario of a SN II. Therefore, extending the early notation of Wasserburg (Lee 1978, Niederer 1980), we would now speak not only about correlated Ca–Ti anomalies, but about correlated overabundances of neutron-rich Ca–Ti–Cr–Fe–Ni–Zn...Zr...Ba–Nd–Sm isotopes in EK-1-4-1.

In full agreement with Meyer, Krishnan and Clayton we conclude that certainly much work remains to be done, although we have also learned a great deal. It will therefore be interesting to see how our insights into FUN syntheses will fit in with future astrophysical models.

### Acknowledgements

Financial support from the German DFG is gratefully acknowledged. The authors thank U. Ott for helpful comments.

### References

- Arlandini et al.: 1999, *Astrophys. J.* **525**, 886.  
Audi G. and Wapstra A.H.: 1993, *Nucl. Phys.* **A565**, 1.  
Balogh W.: 1994, Diploma-Thesis, University of Technology, Vienna.  
Böhmer, W.: 1996, PhD-Thesis, University of Mainz.  
Carraz L.C. et al.: 1982, *Phys. Lett.* **109B**, 419.  
Freiburghaus, C.: 1995, Diploma-Thesis, University Basel.  
Glasmacher T.: 1998, *Ann. Rev. Nucl. Part. Sci.* **48**, 1.  
Glendenning N.K.: 1983, in *Direct Nuclear Reactions* (Academic Press, New York)  
Hillebrandt W. et al.: 1986, in *Weak and Electromagnetic Interactions in Nuclei*, ed. Klapdor H.V.; p. 987.  
Käppeler F. et al.: 1989, *Rep. Prog. Phys.* **52**, 945.  
Kim K.H., Park M.H., Kim B.T.: 1987, *Phys. Rev.* **C23**, 363.  
Kobos A.M., Brown B.A., Lindsay R., Satchler G.R.: 1984, *Nucl. Phys.* **A425**, 205.  
Kratz K.-L., Anne R., Bazin D. et al.: 1991, in *First European Biennial Workshop on Nuclear Physics*, eds. Guinet D. and Pizzi J.R. (World Scientific), p. 218.

- Kratz K.-L. et al.: 1995, *Physikalische Blätter* **51**, 183.
- Krausmann E. et al.: 1996, *Phys. Rev.* **C53**, 469.
- Lee T. et al.: 1978, *Astrophys. J.* **220**, L21.
- Lugmair G.W. et al.: 1978, *Lunar and Planetary Science* **IX**, 672.
- McCulloch M.T. and Wasserburg G.J.: 1978, *Geophysical Research Letters* **5**, 599.
- McCulloch M.T. and Wasserburg G.J.: 1978, *Astrophys. J.* **220**, L15.
- Meyer B.S. et al.: 1996, *Astrophys. J.* **462**, 825.
- Möller P. and Randrup J.: 1990, *Nucl. Phys.* **A514**, 1.
- Möller P., Nix J.R., Myers W.D., Swiatecky W.J.: 1995, *At. Data Nucl. Data Tables* **59**, 185.
- Möller P. et al.: 1997, *Atomic Data Nucl. Data Tables* **66**, 131.
- Niederer, F.R. et al.: 1980, *Astrophys. J.* **240**, L73.
- Oberhummer H. and Staudt G.: 1991, in *Nuclei in the Cosmos*, ed. H. Oberhummer (Springer, Berlin), p. 29.
- Pfeiffer B., Kratz K.-L. and Möller P.: 2000, *Prog. Nucl. Energ.*, in print.
- Rauscher T. et al.: 1995, in *Nuclear Masses and Exotic Nuclei "ENAM'95"*, Edition Frontières, p. 683.
- Rauscher T. et al.: 1998, *Phys. Rev.* **C57**, 2031.
- Sandler D.G., Koonin S.E. and Fowler W.A.: 1982, *Astrophys. J.* **259**, 908.
- Scheit H. et al.: 1996, *Phys. Rev. Lett.* **77**, 3967.
- Sorlin O. et al.: 1993, *Phys. Rev.* **C47**, 2941.
- Sorlin O. et al.: 1995, in *Proc. Nuclei in the Cosmos III*, eds. M. Busso, R. Gallino, C.M. Raiteri (AIP Press, New York), p. 191.
- Thielemann F.-K. et al.: 1979, *Astron. Astrophys.* **74**, 175.
- Thielemann F.-K. et al.: 1990, in *Nuclei in the Cosmos*, eds. Oberhummer H. and Hillebrandt W.; p. 286.
- Wasserburg G.J. et al.: 1977, *Geophys. Res. Letters* **4**, 299.
- Werner T.R. et al.: 1994, *Phys. Lett.* **B333**, 303.
- Ziegert, W.: 1985, PhD-Thesis, University of Mainz.
- Ziegert, W. et al.: 1985, *Phys. Rev. Lett.* **55**, 1935.